CROSS-SECTIONAL SHAPE OF COLLAPSIBLE TUBES

EDWARD KRESCH *and* ABRAHAM NOORDERGRAAF

From The Moore School of Electrical Engineering, University of Pennsylvania, Philadelphia, Pennsylvania 19104

ABSTRACT In order to quantify the collapse phenomenon in veins, this paper presents a mathematical analysis of the cross-sectional shape of a flexible tube as its internal pressure varies. Quantitative results are presented in terms of the physical parameters of the tube, such as wall thickness and Young's modulus. It is assumed that the tube is thin walled, that no stretching occurs, that the cross-sectional shape is elliptical when the transmural pressure is zero, and that the longitudinal prestress is zero. The equations were solved on a digital computer which displayed the cross-sectional shapes on an oscilloscope, which were then photographed. A selection of these photographs is presented. Curves are shown which give the cross-sectional area and compliance as functions of transmural pressure. Other curves are shown which are useful for interpolation, and for use in the experimental determination of the physical parameters which may otherwise be difficult or impossible to measure accurately.

INTRODUCTION

Since the publication in 1628 of William Harvey's classic treatise on circulation, the primary function of veins has been known to be that of returning the blood to the heart. The veins, by virtue of characteristics peculiar to them, play an important role in controlling the output of the heart (Wiggers, 1956; Wood, 1965). This control function of the veins is a passive one, and is a result of their ability to collapse and inflate (Franklin, 1937; Brecher, 1956).

Experimentation on veins in vitro has proceeded slowly because of the nearly insurmountable difficulties involved (Brecher, 1969). The majority of work has been done instead on flexible tubing, based upon the assumption that the differences between them and veins are quantitative in nature rather than qualitative. Holt (1969), Couch (1966), and Conrad (1969) have done such measurements using rubber or plastic tubing. In these experiments, the effects of both positive and negative transmural pressures were investigated.

A certain amount of experimentation has been conducted on veins in vitro in order to determine their Young's modulus (Brecher, 1956; Anliker et al., 1967; Attinger, 1968). It was found that the Young's modulus varies according to the

direction in which it is measured, and according to the extent of stretching. The earliest measurements of changes of cross-sectional shape of veins for varying transmural pressures known to the authors are those made by Attinger (1969). In this work, he restricted himself to positive transmural pressures. Experimental work on both tubes and veins in vitro, using a radiologic technique, have recently been completed by Reddy et al. (1970) for both positive and negative transmural pressures. The cross-sectional shapes they obtained are gratifyingly similar to the curves predicted here.

Recently, Katz and Chen (1970), and Moreno et al. (1970) have presented a theoretical treatment of the collapse phenomenon. Their equations contain the implicit assumption of constant initial (i.e., unloaded) curvature: either a straight piece, like a beam, or a circular cross-section, like a tube. These equations were derived to explain only small gross deformations. Nevertheless, they were amenable to programming on an analogue computer, and any errors resulting from the relatively large gross deformations were apparently small. They were also able to include the effect of stretching in their later calculations, which is important in describing the behavior of veins.

Since the mechanical energy of the blood in veins is extremely small, the veins must be able to accommodate varying amounts of blood with the expenditure of minimal amounts of energy. The ability of veins to collapse provides such a capability. This paper represents a first attempt at quantifying this process. The initial cross-sectional shapes were assumed to be elliptical and the equations were of a form that apply to large gross deformations, but did not include stretching. Being highly nonlinear, the equations were solved using a digital computer. This provided a set of mathematical relationships with which empirical results can be explained. In addition, the results presented here can be extended to predict the dynamic behavior of veins in vivo, to provide a background for the derivation of a mathematical model of the venous system (Kresch and Noordergraaf, 1969), and to guide further experimentation.

DERIVATION OF FORCE AND TORQUE EQUATIONS

The mathematical model which is used is based upon certain assumptions regarding the properties of the tube. These are as follows:

(*a*) The object under consideration is a short segment of a flexible tube. It is assumed that pressure changes along the tube, of which the segment is a part, are sufficiently gradual that end effects can be ignored.

(*b*) The wall thickness h of the tube is sufficiently small that the usual thin-walled approximations can be applied as needed. In particular, if the radius of curvature of the cross-section is ρ, then at all points on the boundary, in both initial shape and in all subsequent shapes after deformation, it may be assumed that:

$$h \ll \rho. \tag{1}$$

(*c*) The velocities of the wall are assumed to be sufficiently small so that energy losses due to heating in the wall, and energy storage due to the inertia of the wall, may be safely ignored.

(*d*) The transmural pressures under consideration are assumed to be small enough that no appreciable stretching occurs in the wall.

(*e*) The cross-sectional shape of the tube, when the transmural pressure is zero, is assumed to be elliptical.

(*f*) The wall thickness is assumed to be constant.

(*g*) The wall is assumed to be homogenous, but not necessarily isotropic.

(*h*) The cross-sectional shape of the tube is symmetrical about both axes.

(*i*) The longitudinal prestress is zero.

The tube to be considered is unbranched, straight, of infinite length, and has a cross-section which does not change along its length, and a suitable piece of this tube is chosen for analysis. This is the mathematical equivalent of a tube of finite length without end effects. The piece chosen is shown schematically in Fig. 1.

The various parameters are defined in Fig. 2. The wall thickness h is assumed to be a constant, independent of position on the wall. The transmural pressure p is defined as the amount by which the internal pressure exceeds the external pressure, and may take on negative values. It is useful to consider the forces and torques acting upon this piece of the tube wall.

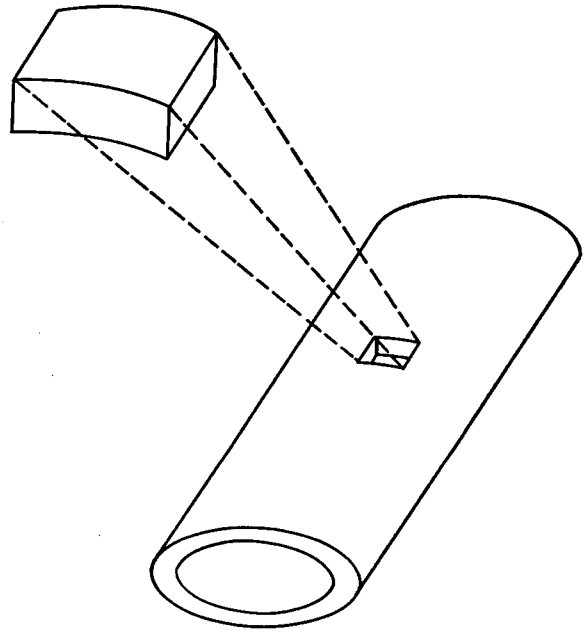

FIGURE 1 A section of flexible tube and a piece of the tube used in the derivation of the shape equation.

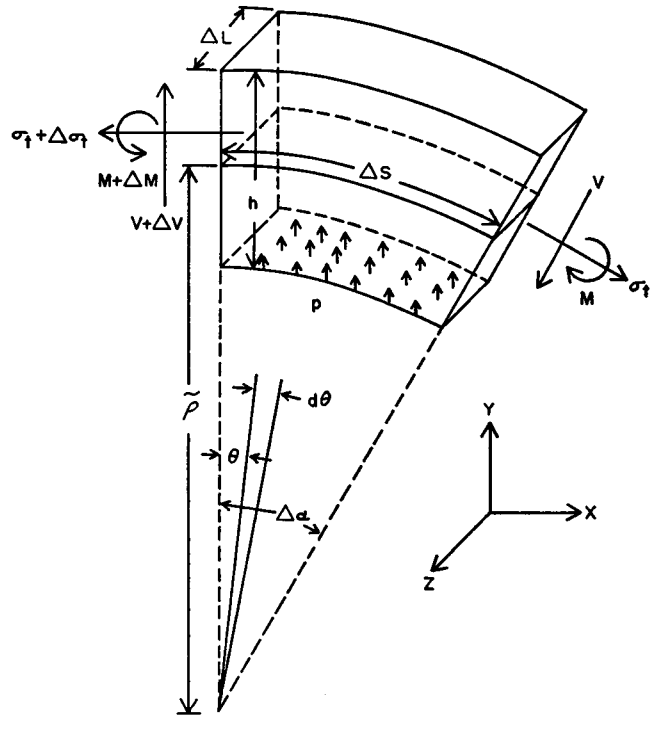

FIGURE 2 A small wedge-shaped piece of tube obtained as shown in Fig. 1. In addition to the thickness h and the length ΔL, the width is shown to be defined as the arc length of the midline. An approximation to the radius of curvature ρ is defined geometrically, denoted by $\tilde{\rho}$. The tangential stress σ_t, the shear V, and the bending moment M are shown acting on the right-hand face. On the left-hand face, these same variables are shown with incremented values. The transmural pressure p is shown acting on the inside face. In addition, a set of reference axes is shown.

Since the wall is in static equilibrium, the sum of the forces acting on it in any direction must be equal to zero, as must the sum of the torques about any axis. A consideration of the forces acting in the y-direction yields:

$$(V + \Delta V)\Delta Lh - V\Delta Lh \cos \Delta\alpha + \int_0^{\Delta\alpha} p\Delta L\left(\tilde{\rho} - \frac{h}{2}\right)\cos\theta \, d\theta - \sigma_t \Delta Lh \sin \Delta\alpha = 0, \quad (2\,a)$$

and a consideration of the torque about a line in the y-direction and passing through a point located at the center of the left-hand face yields:

$$(M + \Delta M)\Delta Lh - M\Delta Lh - \tilde{\rho}V\Delta Lh - \tilde{\rho}V\Delta Lh \tan \Delta\alpha + \int_0^{\Delta\alpha} p\Delta L\left(\tilde{\rho} - \frac{h}{2}\right)^2 \tan\theta \, d\theta = 0. \quad (2\,b)$$

Using approximation 1 above, and taking the limit as $\Delta s \to 0$ gives:

$$h\dot{V} + p - \sigma_t \kappa h = 0, \tag{3 a}$$

$$\dot{M} = V. \tag{3 b}$$

Combining these two equations gives:

$$h\ddot{M} + p - \sigma_t \kappa h = 0. \tag{3 c}$$

In the above equations, dots are used to indicate differentiation with respect to s, and κ is the curvature at any point defined by:

$$\kappa = \frac{1}{\rho}, \tag{4 a}$$

and

$$\lim_{\Delta s \to 0} \tilde{\rho} = \rho. \tag{4 b}$$

In the case where the shear V is constant, equation 3 a reduces to Laplace's law. It will be shown below that the condition for which the shear is constant is that the cross-section be circular. Equation 3 c is the equation which is to be solved in order to determine the cross-sectional shapes of collapsible tubes.

EXPRESSIONS FOR FORCE AND TORQUE AS RELATED TO STRESS AND BENDING MOMENT

An expression for force can be most easily determined by considering the behavior of a slice of the tube as shown in Fig. 3. If this slice is cut symmetrically into two equal halves, the resulting situation will be as is shown in Figure 4. The two points where it was cut have as coordinates (x_1, y_1) and (x_2, y_2). By symmetry, it must be true that $x_2 = -x_1$ and $y_2 = -y_1$. The coordinates of the curve, x and y, are expressed parametrically in terms of the arc length s. The point where the curve intersects the positive x-axis defines where s is equal to zero, with s increasing in a counterclockwise direction. The point (x_1, y_1) is located at $s = s_1$, and the point (x_2, y_2) is located at $s = s_2$. The tangential stress σ_{t1}, the shear V_1, and the bending moment M_1 act at the point (x_1, y_1), and equivalently for σ_{t2}, V_2, and M_2 at (x_2, y_2). As above, pressure is measured relative to the external pressure, so no external pressure is shown. The internal pressure is arbitrarily shown acting in an outward direction.

It is demonstrated below that the bending moment at any point M depends only on the curvature at that point, and on the transverse Young's modulus and the wall thickness, both of which are assumed to be constant. By symmetry, the curvature at (x_1, y_1) must equal the curvature at (x_2, y_2), implying the equality of the

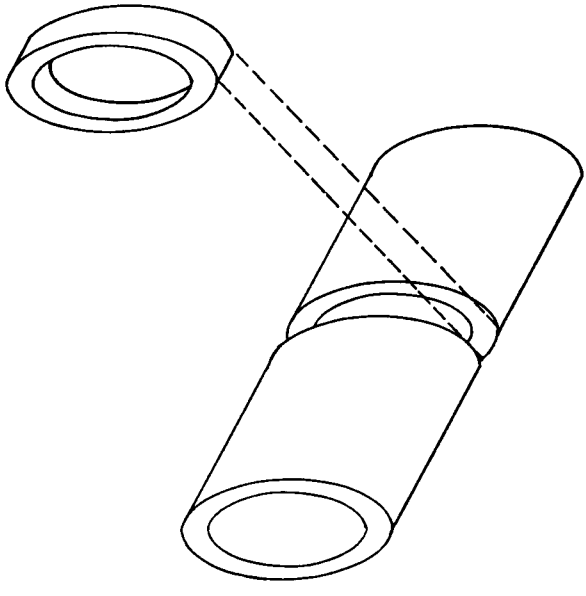

FIGURE 3

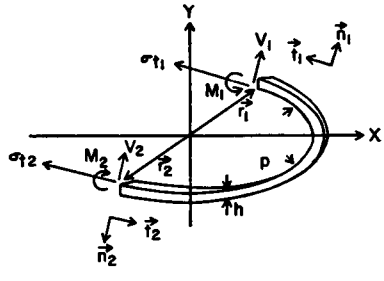

FIGURE 4

FIGURE 3 A section of flexible tube and a slice of the tube used in the derivation of the expressions for stress and shear.

FIGURE 4 In order to determine the tangential stress σ_t and the shear V, the ring-shaped slice of Fig. 3 is cut in half at symmetrically opposite points. The tangential stress σ_t, the shear V, and the bending moment M are shown acting at the two points where it is cut, and the transmural pressure p is shown acting in an outward direction. At each point on the ring are associated three vectors: the position vector **r**, which locates the point relative to the origin of coordinates; the unit tangent vector **t**, which is parallel to the ring and points in the direction of increasing arc length; and the unit outward normal **n**. These vectors are shown at the two symmetrical points.

bending moments at the two points. By virtue of equation 3 *b* above, therefore,

$$V_1 = V_2 \,(= V). \tag{5}$$

Symmetry arguments also require that:

$$\mathbf{r}_1 = -\mathbf{r}_2\,, \tag{6 a}$$

$$\mathbf{t}_1 = -\mathbf{t}_2\,, \tag{6 b}$$

$$\mathbf{n}_1 = -\mathbf{n}_2\,. \tag{6 c}$$

In addition, the following mathematical definitions are needed:

$$\mathbf{r} = x\mathbf{i} + y\mathbf{j}, \tag{7 a}$$

$$\mathbf{t} = \dot{x}\mathbf{i} + \dot{y}\mathbf{j}, \tag{7 b}$$

$$\mathbf{n} = \dot{y}\mathbf{i} - \dot{x}\mathbf{j}, \tag{7 c}$$

where $\mathbf{i}$ and $\mathbf{j}$ are unit vectors in the x- and y-directions respectively. The appropriate expressions for $\mathbf{r}_1$, $\mathbf{t}_1$, etc. should be obvious.

Three quantities are of interest: the net torque $\mathbf{T}$ about the z-axis, the net force component F_t in the $\mathbf{t}_1$ direction, and the net force component F_n in the $\mathbf{n}_1$ direction, all of which must be equal to zero. These quantities are:

$$\mathbf{T} = \mathbf{r}_1 \times (V_1 \Delta Lh\mathbf{n}_1) + \mathbf{r}_2 \times (-V_2 \Delta Lh\mathbf{n}_2) + \mathbf{r}_1 \times (\sigma_{t1} \Delta Lh\mathbf{t}_1) + \mathbf{r}_2 \times (-\sigma_{t2} \Delta Lh\mathbf{t}_2) + \int_{(x_2,y_2)}^{(x_1,y_1)} \mathbf{r} \times (\Delta Lp\mathbf{n}\, ds) = 0, \quad (8\,a)$$

$$F_t = V_1 \Delta Lh\mathbf{n}_1 \cdot \mathbf{t}_1 - V_2 \Delta Lh\mathbf{n}_2 \cdot \mathbf{t}_2 + \sigma_{t1} \Delta Lh\mathbf{t}_1 \cdot \mathbf{t}_1 - \sigma_{t2} \Delta Lh\mathbf{t}_2 \cdot \mathbf{t}_1 + \int_{(x_2,y_2)}^{(x_1,y_1)} \Delta Lp\mathbf{n} \cdot \mathbf{n}_1\, ds = 0, \quad (8\,b)$$

$$F_n = V_1 \Delta Lh\mathbf{n}_1 \cdot \mathbf{n}_1 - V_2 \Delta Lh\mathbf{n}_2 \cdot \mathbf{n}_1 + \sigma_{t1} \Delta Lh\mathbf{t}_1 \cdot \mathbf{n}_1 - \sigma_{t2} \Delta Lh\mathbf{t}_2 \cdot \mathbf{n}_1 + \int_{(x_2,y_2)}^{(x_1,y_1)} \Delta Lp\mathbf{n} \cdot \mathbf{n}_1\, ds = 0. \quad (8\,c)$$

When the conditions required by equations 5–7 are substituted into equation 8 *a*, it reduces to:

$$\sigma_{t1} = \sigma_{t2}\ (=\sigma_t). \quad (9)$$

Equations 8 *b* and 8 *c* then yield, respectively:

$$\sigma_t = \frac{p}{h}(x\dot{y} - \dot{x}y), \quad (10)$$

$$V = -\frac{p}{h}(x\dot{x} + y\dot{y}). \quad (11)$$

In order to enhance insight, it is worthwhile to make a digression at this point. A consideration of equations 3 *a*, 3 *b*, 10, and 11 yields several interesting results. In the notation used in this paper, Laplace's law has the form:

$$p = \frac{\sigma_t h}{\rho}, \quad (12)$$

in which the tension, usually denoted by τ, is replaced by its mathematical equivalent $\sigma_t h$, and the radius of curvature ρ replaces the radius, since the cross-section is not necessarily circular. Consider the following statements:

(*a*) Laplace's law holds.

(*b*) The shear is constant.

(*c*) The shear is identically zero.
(*d*) The cross-section is circular.
(*e*) The stress is constant.
(*f*) The bending moment is constant.
(*g*) The curvature is constant.

It is not difficult to show that these seven statements are mathematically synonymous, in the sense that they are either all true or all false. This is not to imply that the above seven statements must be true; in the case of a collapsed vein, for example, statement *d* is certainly not true. The important point is that if any one of the above statements is false, all the others must also be false.

In particular, equation 12 is not necessarily correct. It may be noticed that equation 10, which is necessarily correct, is identical with equation 12 except that the radius of curvature ρ is replaced by the quantity $x\dot{y} - \dot{x}y$. Thus, equation 10 is one form of a generalization to Laplace's law for noncircular cross-section. In the case of circular cross-section, equations 10 and 12 become indistinguishable. Another generalization of Laplace's law is given by equation 3 *c*. Except for the addition of the term $h\ddot{M}$, this is identical with equation 12.

It should be no surprise that all these equations are intimately related. For example, it is possible to derive equation 3 *a* by differentiating equation 11 and, making use of equations 10, 18, and 19, performing a certain amount of mathematical manipulation.

AN EXPRESSION FOR THE BENDING MOMENT

Knowing that the cross-section may not be circular, it is necessary to determine what the actual shape is. The starting point is equation 3 *c*, which is the basic force relationship for the system. Since equation 11, which is mathematically equivalent to equation 3 *c*, provides a more convenient starting point, the shape will be determined by solving equation 11. The first step in this solution is to integrate this equation along the arc length from the point $s = 0$ to an arbitrary point on the circumference:

$$M - M(0) = -\frac{p}{2h}(x^2 + y^2) + \frac{p}{2h}x(0)^2, \tag{13}$$

where $M(0)$ and $x(0)$ are the values of M and x at the point $s = 0$. This, as defined above, is the intersection of the curve with the positive x-axis, which means that $y(0) = 0$. It is necessary now to determine an expression which gives the bending moment in terms of the physical properties of the tube.

An expression for the bending moment in terms of the curvature can be obtained from a consideration of the piece of tube shown in Fig. 2. Fig. 5 shows this same piece of tube as it might appear (*a*) when the bending moment is zero, and (*b*) when the bending moment is equal to some nonzero value M, shown in the figure as a

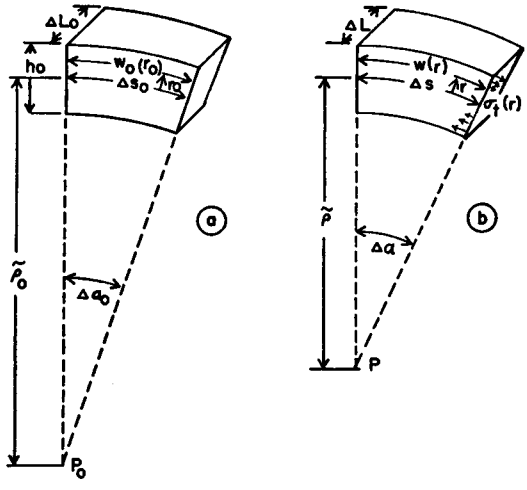

FIGURE 5

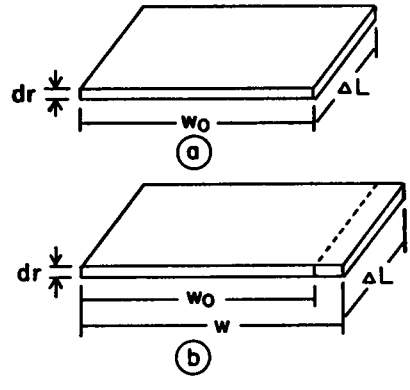

FIGURE 6

FIGURE 5 The wedge-shaped piece of tube of Fig. 2 in two states. In *a* it is shown as it appears when no forces or torques act on it. The geometric variables are shown with a zero subscript to indicate that they apply to the state for force and torque equal to zero. The width is denoted by w_0 which, as illustrated, is a function of the radial distance r_0. When $r_0 = 0$, the width w_0 is equal to the center-line width Δs_0. In *b* the same piece of tube is shown as it appears when the forces and torques are allowed to act on it. The geometric variables are shown without a subscript. The only force shown is that due to the tangential stress σ_t in order to emphasize that it varies with r.

FIGURE 6 The wedge-shaped piece of tube shown in Fig. 5 *a* is cut into layers of thickness dr. Such a layer is shown in *a*. When the forces and torques are applied, the layer is deformed, and appears as shown in *b*.

positive quantity. From this figure, it is possible to determine a strain and a stress, and to relate them through Young's modulus.

If the piece of tube shown in Fig. 5 *a* is divided into a series of thin horizontal layers, one of these layers might appear as shown in Fig. 6 *a*. In this figure, the slab is shown as being flat, rather than curved, which makes it easier to visualize what is happening. When the bending moment is applied the width w_0 of this slab may change. It is shown in Fig. 6 *b* as having increased. The strain ϵ as a function of the radial coordinate r is given by:

$$\epsilon = \frac{1 + \tilde{\kappa} r}{1 + \tilde{\kappa}_0 r} - 1. \tag{14}$$

The stress is obtained by multiplying this by the transverse Young's modulus E_t. The torque about the midline of the right-hand face is given by the formula:

$$T = \int_{-h/2}^{h/2} r E_t \epsilon(r) \Delta L \, dr. \tag{15}$$

The bending moment is the torque per unit area. Integrating equation 15 and dividing by the area ΔLh, gives the bending moment:

$$M = (\kappa - \kappa_0)\frac{E_t}{\kappa_0^2}\left[\frac{1}{h\kappa_0}\ln\frac{1+\frac{1}{2}h\kappa_0}{1-\frac{1}{2}h\kappa_0} - 1\right]. \tag{16}$$

This equation states that at any point on the tube, the bending moment is linearly proportional to the change in curvature at that point. Since the cross-section for zero transmural pressure is not necessarily circular, the curvature κ_0 is not constant, so that the proportionality factor varies from point to point. As long as the wall thickness is small relative to the radius of curvature, however, the factor does not vary much, so that the following approximation can be used:

$$M \approx \tfrac{1}{12}E_t h^2(\kappa - \kappa_0). \tag{17}$$

AN EXPRESSION FOR THE ARC LENGTH

The arc length of a curve is defined by the equation:

$$ds^2 = dx^2 + dy^2, \tag{18}$$

where s is the arc length, and x and y are the x- and y-coordinates of the curve, respectively, where x and y are expressed parametrically in terms of the arc length. In actual fact, there are two curves of interest: that for which the transmural pressure is zero, and that for which the pressure is not zero. The first curve is given; the second is to be determined. If s_0 is any point in the cross-section described by the first curve, then its coordinates are $x_0(s_0)$ and $y_0(s_0)$. Let s be the same physical point in the cross-section after the pressure is made nonzero. In a general situation where stretching is allowed, s and s_0 need not be equal. In this case, since stretching is so slight as to be negligible, it can be assumed that $s = s_0$. Thus, the point defined by s at one value of transmural pressure is the same physical point at all values of transmural pressure.

AN EXPRESSION FOR THE CURVATURE

An expression for the curvature κ is easy to derive. The curvature, defined as the inverse of the radius of curvature, is the rate of change with respect to arc length of the angle between the line tangent to the curve and the x-axis. When this is translated into cartesian coordinates, the result is:

$$\kappa = \dot{x}\ddot{y} - \ddot{x}\dot{y}. \tag{19}$$

A METHOD FOR FINDING A CURVE FROM ITS CURVATURE

It will be necessary later to determine the coordinates of a curve given only its curvature as a function of arc length $\kappa(s)$ and its initial conditions. It is necessary to determine a method for doing this, and to determine which initial conditions must be specified. These determinations are easily made by defining a dummy variable θ according to the following two equations:

$$\dot{x} = -\sin\theta, \tag{20 a}$$

$$\dot{y} = \cos\theta. \tag{20 b}$$

When these are differentiated and substituted into equation 19, the result is:

$$\dot{\theta} = \kappa. \tag{20 c}$$

Equations 20 *a*–20 *c* can be integrated:

$$\theta = \theta(0) + \int_0^s \kappa \, ds, \tag{21 a}$$

$$x = x(0) - \int_0^s \sin\theta \, ds, \tag{21 b}$$

$$y = y(0) + \int_0^s \cos\theta \, ds. \tag{21 c}$$

These equations show that there are three initial conditions which must be specified. $x(0)$ and $y(0)$ give the location of the point where $s = 0$, and $\theta(0)$ is related to the slope of the curve at this point. These equations also provide the basis for a method of integration for use in a digital computer.

RESTING SHAPE OF THE TUBE

It is necessary to specify the "resting shape," the cross-sectional shape when the transmural pressure is zero, assuming that the bending moment is at all points zero. The first impulse is to define the resting shape as circular. There are two reasons why this was not done.

(*a*) Although perfect circles do not exist in nature, mathematically just the opposite is true. By virtue of its perfect symmetry, a circular cross-section will never collapse, regardless of the extent by which the external pressure exceeds the internal pressure. In reality, it is the slight perturbations from perfection that cause flexible tubes to collapse. Mathematically, a similar perturbation must be introduced or the equations yield trivial results.

(*b*) The actual resting shape of veins is not known, so that making the assumption that they are circular may be physiologically in error.

Consequently, it is assumed that the resting cross-sections are elliptical. The eccentricity k is defined here (this is not the usual definition of eccentricity) as the ratio of the major axis to the minor axis. It should be clear that as good an approximation to a circle as required can be obtained by making the eccentricity sufficiently close to unity. The equation of such an ellipse is:

$$x_0^2 + k^2 y_0^2 = 1, \tag{22}$$

where the subscripts indicate that this is for transmural pressure equal to zero. It is not possible to write an analytic expression which gives these coordinates as functions of the arc length. In order to obtain a computer solution, the curvature κ_0 is written as:

$$\kappa_0 = \frac{(\dot{x}_0^2 + k^2 \dot{y}_0^2)^{3/2}}{k}, \tag{23}$$

and the necessary functions are then given by:

$$\dot{x}_0 = \dot{x}_0(0) - \int_0^s \kappa_0 \dot{y}_0 \, ds, \tag{24 a}$$

$$\dot{y}_0 = \dot{y}_0(0) + \int_0^s \kappa_0 \dot{x}_0 \, ds. \tag{24 b}$$

This requires two initial conditions:

$$\dot{x}_0(0) = 0, \tag{25 a}$$

$$\dot{y}_0(0) = 1. \tag{25 b}$$

The original shape equation 3 *c* has now been replaced by a set of five first-order differential equations, three to determine the curve from its curvature and two to determine the ellipse.

SOLUTION AND RESULTS

Whenever it is possible to express a set of simultaneous differential equations in the form:

$$\dot{u} = f(u, s), \tag{26}$$

where u, $\dot{u}(= du/ds)$, and f are vectors, it is possible to write a computer program which will approximate the value of $u(s + \Delta s)$ from the behavior of $u(s)$, $u(s - \Delta s)$,

$u(s - 2\Delta s)$, etc. Equations 13, 17, 20 *a*–20 *c*, and 24 *a*–24 *b* can be put in the above form as follows:

$$\begin{bmatrix} \dot{\theta} \\ \dot{x} \\ \dot{y} \\ \ddot{x}_0 \\ \ddot{y}_0 \end{bmatrix} = \begin{bmatrix} -P(x^2 + y^2) - Px(0)^2 + \dot{\theta}(0) + \dfrac{(\dot{x}_0^2 + k^2\dot{y}_0^2)^{3/2}}{k} - k^2 \\ -\sin\theta \\ \cos\theta \\ -\dot{y}_0 \dfrac{(\dot{x}_0^2 + k^2\dot{y}_0^2)^{3/2}}{k} \\ \dot{x}_0 \dfrac{(\dot{x}_0^2 + k^2\dot{y}_0^2)^{3/2}}{k} \end{bmatrix}, \quad (27)$$

where P is the normalized pressure and replaces $6p/E_t h^3$. The initial conditions for this set of equations are:

$$\begin{bmatrix} \theta(0) \\ x(0) \\ y(0) \\ \dot{x}_0(0) \\ \dot{y}_0(0) \end{bmatrix} = \begin{bmatrix} 0 \\ x_i \\ 0 \\ 0 \\ 1 \end{bmatrix}. \quad (28)$$

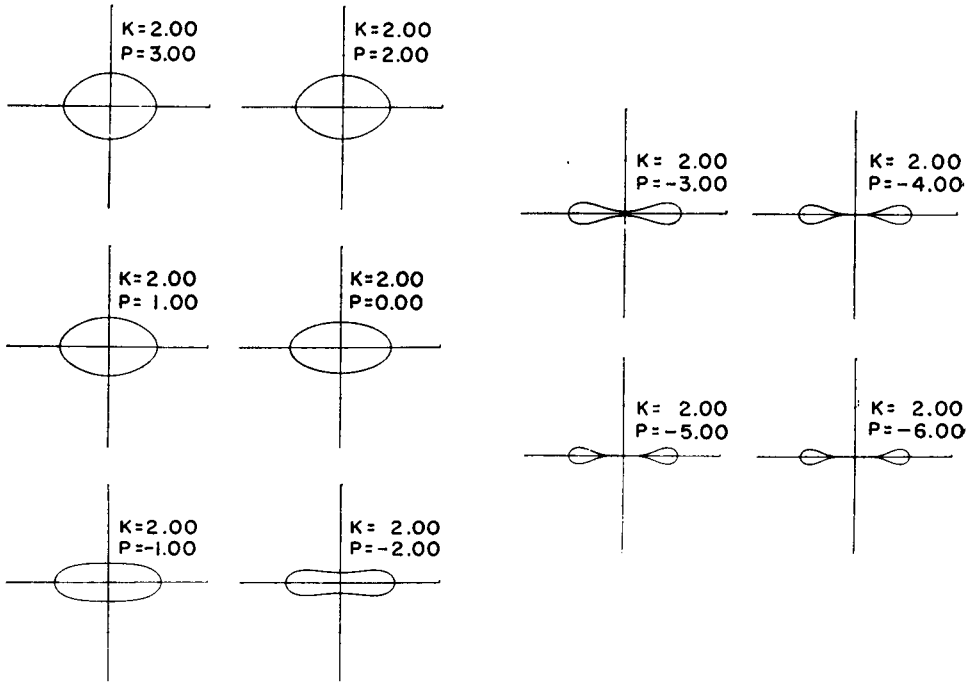

FIGURE 7 A sequence of photographs of a computer-controlled oscilloscope showing a sequence of computed cross-sectional shapes. The shape for transmural pressure equal to zero was assumed to be an ellipse with an eccentricity $k = 2.0$ for this sequence. The normalized pressure P ranges from $+3.0$ to -6.0 in steps of -1.0.

It should be noted that equation 13 was derived through an integration, which gave rise to a sixth initial value, $\dot{\theta}(0) = \dot{\theta}_i$. The integration is to be carried out through one-fourth the arc length of the cross-section. Since the cross-section is known to be symmetric about both axes, this is sufficient. Although x_i and $\dot{\theta}_i$ are not known, the correct values of $x(s)$ and $\dot{y}(s)$ are known to be zero at the end point of the integration. What was done was to guess at the values of x_i and $\dot{\theta}_i$, , then to compute the curve for this cross-section and examine the values of $x(s)$ and $\dot{y}(s)$ actually obtained at the end point. These values, if not both correct, allowed the computer to generate a better approximation to x_i and $\dot{\theta}_i$. The process used caused a rapid convergence of x_i and $\dot{\theta}_i$ to their correct values.

The equations were solved for five values of the eccentricity k: 2.0, 1.5, 1.25, 1.125, and 1.0625. For each value, the normalized pressure P was varied, starting at $+3.0$ and ending at -6.0 in steps of -0.2. A selection of the curves so obtained is shown in Fig. 7, for which $k = 2.0$. Other curves have been published by Kresch (1968).

In addition to computing the cross-sectional shape, the area was also calculated. Plots of the cross-sectional area as a function of the normalized pressure are shown in Fig. 8 for the five values of eccentricity, and for an extrapolation to the limit as

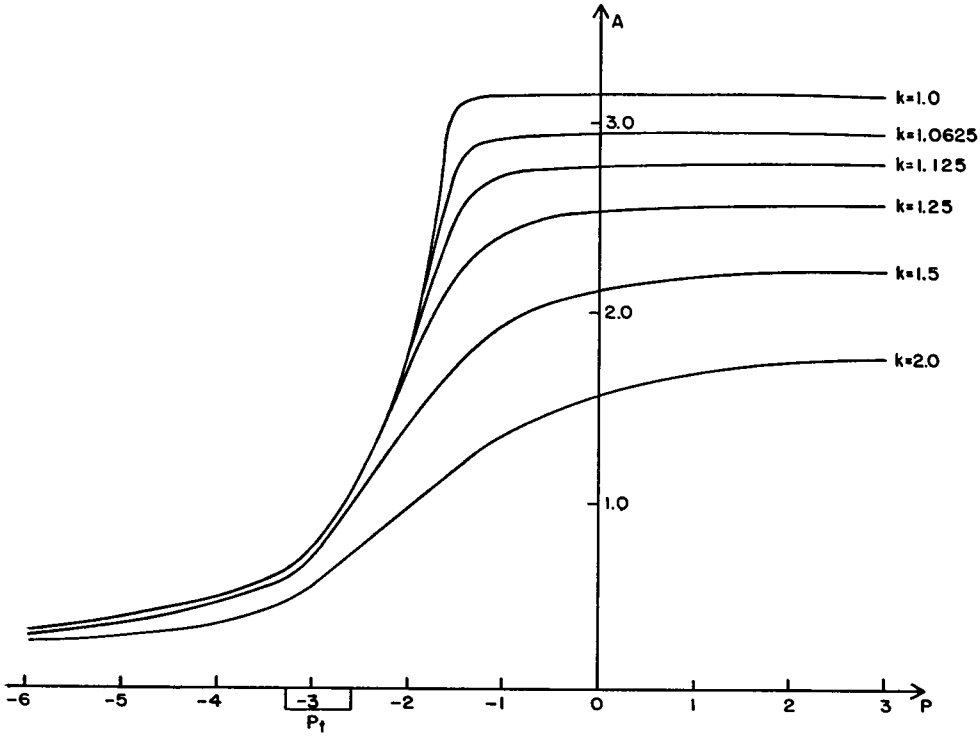

FIGURE 8 A composite graph of the cross-sectional area A as a function of the transmural pressure P for six values of initial eccentricity k.

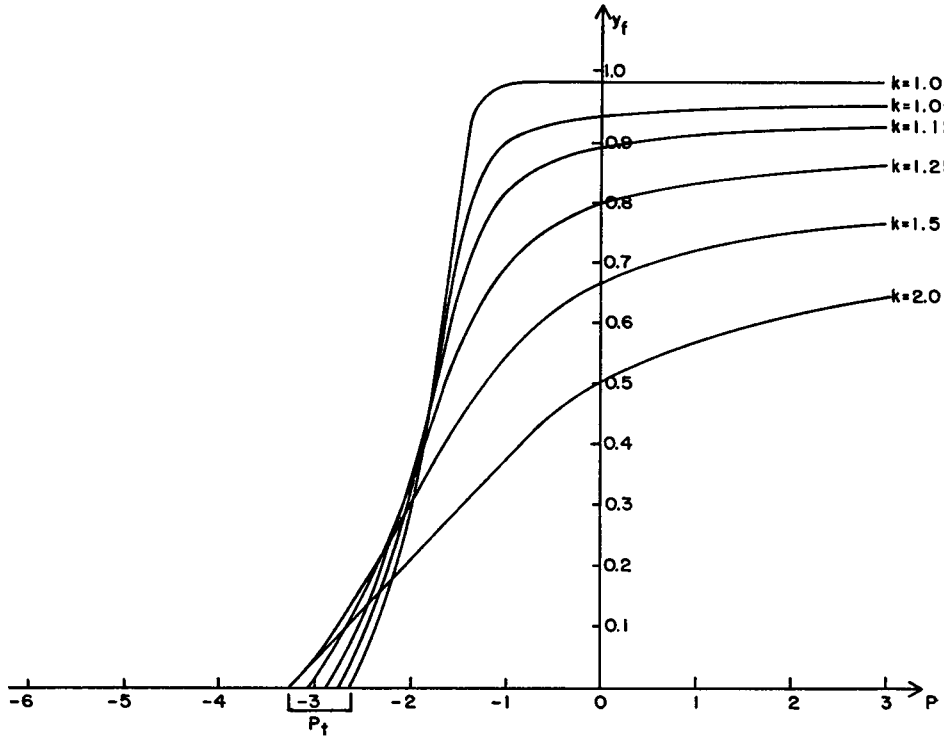

FIGURE 9 A composite graph of the y-axis intercept y_f as a function of the transmural pressure P for six values of initial eccentricity k.

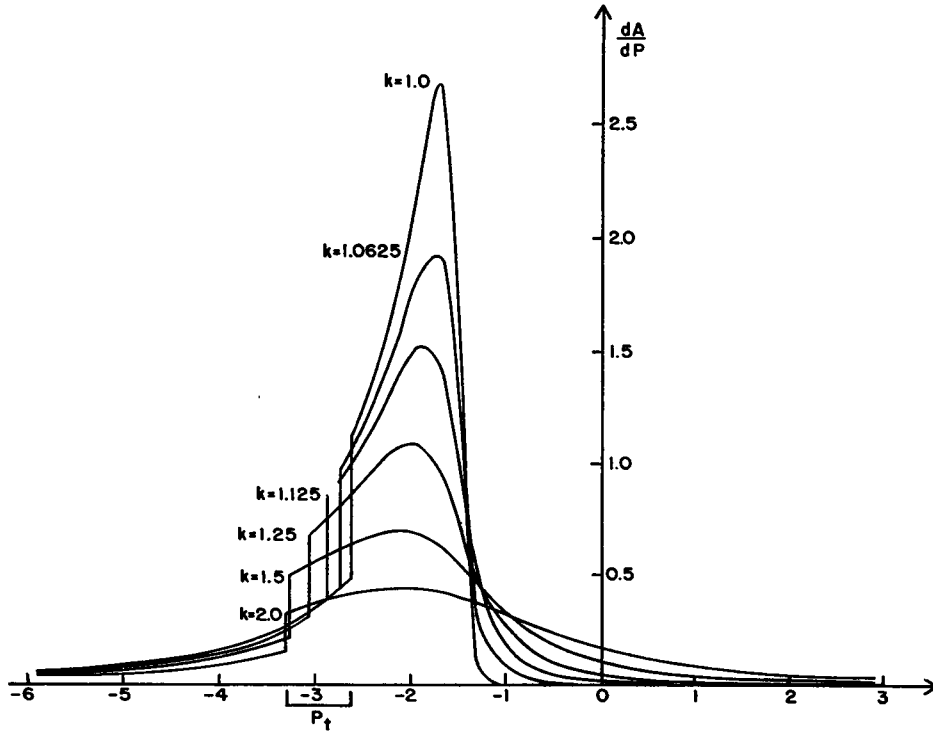

FIGURE 10 A composite graph of the compliance dA/dP as a function of the transmural pressure P for six values of initial eccentricity k. Each of these curves has a discontinuity at $P = P_t$. Since P_t itself varies as a function of the initial eccentricity, the discontinuities occur at different places for the six curves.

the eccentricity approaches unity. Graphs of the y-intercept y_f and for the normalized compliance dA/dP are shown as functions of the normalized pressure in Figs. 9 and 10 respectively.

From Fig. 9, it is possible to estimate the value of the normalized pressure at which the top and bottom walls of the tube touch, being the value of P at which y_f goes to zero. This value of pressure, denoted by P_t, is plotted as a function of the eccentricity k in Fig. 11. For this range of k, P_t increases for larger eccentricity. This implies that the flatter curves require larger pressures to cause the walls to touch. This apparent paradox results from the unusual form of normalization used here: setting the major axis equal to unity. A larger eccentricity thus implies a lesser perimeter, and hence less material over which to distribute the flexural forces. For even larger eccentricity, however, it can be speculated that the proximity of the upper and lower walls will more than compensate for this effect.

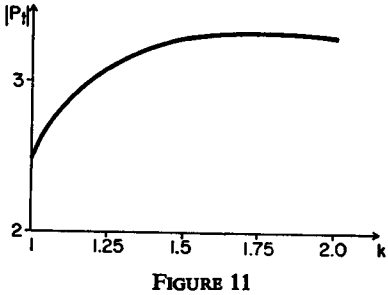

FIGURE 11

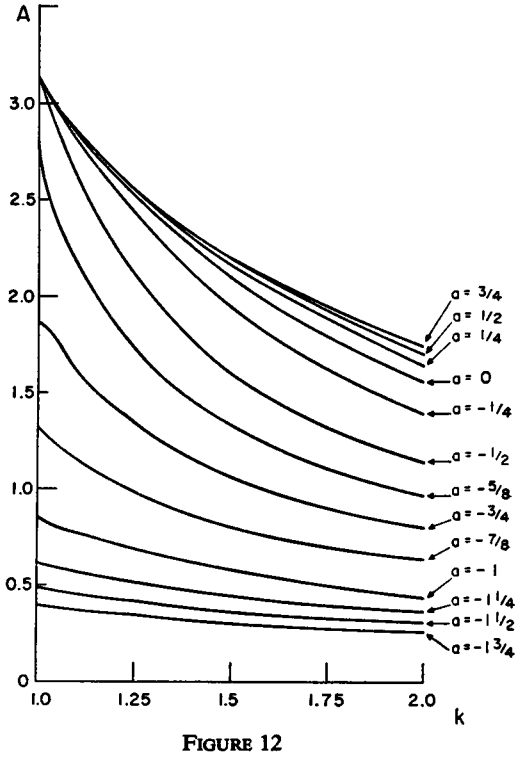

FIGURE 12

FIGURE 11 A graph showing the value of normalized transmural pressure where the walls touch P_t as a function of the initial eccentricity k. For the range of eccentricities considered, $|P_t|$ increases as k increases, implying that the closer the walls are initially, the greater the pressure needed to make them touch. This apparent contradiction is a result of the normalization procedure used. It can be speculated that, for values of k larger than those considered here, $|P_t|$ decreases.

FIGURE 12 A composite graph showing the cross-sectional area A as a function of the initial eccentricity k for 13 values of the parameter a, defined as the ratio $P/|P_t|$.

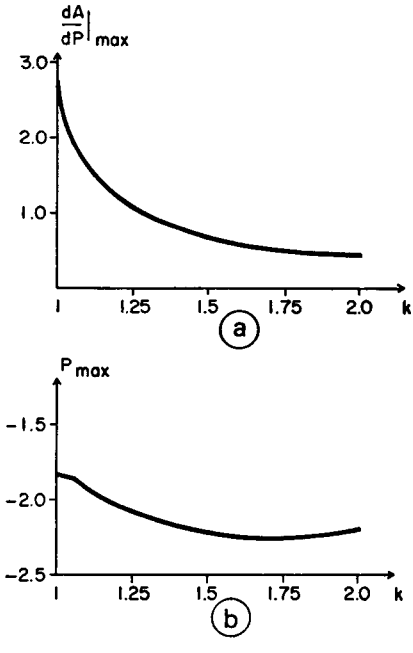

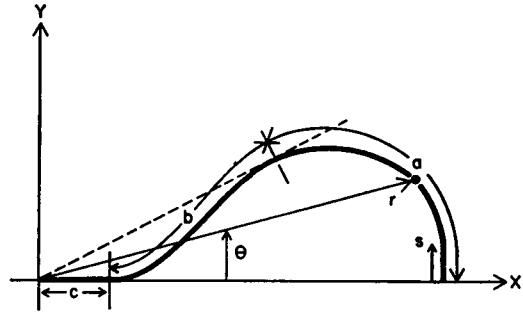

FIGURE 13

FIGURE 14

FIGURE 13 (*a*) A graph of the maximum value of the compliance $dA/dP|_{max}$ as a function of the initial eccentricity k. (*b*) A graph of the normalized transmural pressure P_{max}, at which the maximum value of compliance occurs, as a function of k.

FIGURE 14 One quadrant of a partially collapsed tube. In cylindrical coordinates, every point of the tube (black dot) is uniquely identified by a radial coordinate r and an angle θ defined as shown. The arc length s is shown increasing in a counterclockwise direction. Three sections of the wall are identified: *a*, *b*, and *c*. In *a*, $\dot{\theta}$ is positive; in *b*, θ is negative; and in *c*, $\dot{\theta}$ is identically zero. The boundary point between *a* and *b* is where a line from the origin of coordinates is tangent to the curve (dashed line); that between *b* and *c* is where the curve touches the x-axis.

Fig. 12 is a composite graph showing the behavior of the cross-sectional area as a function of the eccentricity k. Each value of k determines the value of P_t. For that eccentricity, the actual normalized transmural pressure is expressed as:

$$P = a \mid P_t \mid, \tag{29}$$

where a is a dimensionless factor. Each curve on Fig. 12 is for constant a. For example, to find the cross-sectional area of the tube when the top and bottom touch, look at the curve for $a = -1$. This gives the area for all values of eccentricity up to 2. This figure is presented in order to facilitate interpolation between the values of k for which the equations were solved.

Fig. 13 *a* is a graph of the maximum value of the compliance, $dA/dP|_m$, and Fig. 13 *b* is a graph of the value of P at which the maximum occurs, P_m, both as functions of k.

CONCLUSIONS

Clearly, one of the main reasons for presenting this paper is to provide a theoretical foundation describing the collapse of flexible tubes which can be used as a basis for comparison with experimental work. In making measurements on flexible tubes or veins, curves similar to those shown above will be obtained. In order to make such a comparison, it is necessary to explain the relationship between the curves shown above, and the units for curves experimentally obtained. This must be done in order to compensate for the size of the vessel or tube, and to obtain a relationship between the normalized pressure P and the actual transmural pressure p expressed in engineering units.

In deriving the equations for this paper, the major axis[1] for zero transmural pressure was defined as unity. This defines a unit of length. The wall thickness was defined as h in terms of these units. The following relationships can be shown to hold:

$$h = \frac{h'}{x_a}, \tag{30 a}$$

$$A = \frac{A'}{x_a^2}, \tag{30 b}$$

$$P = \frac{6p}{E_t h^3}, \tag{30 c}$$

$$\frac{\mathrm{d}A}{\mathrm{d}P} = \frac{E_t h^3}{6x_a^2}\frac{\mathrm{d}A'}{\mathrm{d}p}, \tag{30 d}$$

$$y_f = \frac{y_f'}{x_a}, \tag{30 e}$$

where:

h' is the actual measured wall thickness of the tube,

A' is the actual measured cross-sectional area of the tube,

x_a is the actual measured x-axis intercept of the tube for zero transmural pressure, and

y_f' is the actual measured y-axis intercept of the tube.

The quantity $1/12\ E_t h^3$ is an important descriptor of the behavior of the wall of the tube. Multiplication of equation 17 by the wall thickness h shows that $1/12\ E_t h^3$ is the proportionality factor relating the torque per unit (axial) length of the tube to the change in curvature. It is a rotational analogy of the spring constant in Hooke's law, which we shall call the bending modulus and denote by the letter c.

The bending modulus is difficult to measure directly. The considerations presented in this paper provide for a variety of procedures for determining the value of the

[1] Note that the major axis, as used here, is the distance from the origin to the x-intercept.

bending modulus indirectly, depending upon what measurements are made. One such procedure is described here. It is assumed that the tube has been set up so that the transmural pressure p can be controlled and the volume of the tube can be determined at all times.

The major axis $x(0)$ varies only slightly as a function of the transmural pressure. It should not be difficult to measure $x(0)$ when the transmural pressure is approximately equal to zero. This gives a value for x_a. A glance at the curves of Fig. 8 shows that, when $p \approx 0$, the cross-sectional area also varies only slightly as a function of the transmural pressure, so that a measurement of the volume gives, upon division by the length of the tube, an accurate value for $A'(0)$. The normalized area $A(0)$ can be obtained, according to equation 30 b, by dividing $A'(0)$ by x_a^2. Referring to Fig. 12, the curve for $a = 0$ gives the eccentricity k which is valid for the value of A obtained (the direct determination of the eccentricity requires accurate control over the transmural pressure to a degree which may not be available). Once the eccentricity is known, the value of $| P_t |$ can be read directly from Fig. 11.

The value of transmural pressure at which the walls touch p_t may be determined in a variety of ways. One possibility is to apply a slow sinusoidal oscillation of low amplitude about a value of transmural pressure and determine the resultant amplitude of volume (and, hence, cross-sectional area) change. It will be noticed, from Fig. 10, that $\mathrm{d}A/\mathrm{d}P$ undergoes a discontinuity at $p = p_t$. Therefore, if the resting value is slowly changed, an abrupt change in the amplitude of the volume oscillation will be noted as p passes through p_t. The value of transmural pressure when this occurs can be taken as p_t. It may be noted, from equation 30 c, that:

$$c = \frac{p_t}{2P_t}, \tag{31}$$

which is the quantity required.

It may be reasoned that the bending modulus should be quite easy to obtain; it can be calculated easily once the wall thickness and the transverse Young's modulus are known. The fallacy with this sort of reasoning is that the transverse Young's modulus is not easily measured on plastic tubing, and is extremely difficult to measure on veins. In fact, one of the key reasons for determining the bending modulus indirectly, as described above, is that a relatively accurate value for the transverse Young's modulus may then easily be determined by multiplying it by $12/h^3$, assuming that the wall thickness h is not difficult to measure accurately.

A parameter of interest, particularly to hemodynamicists, is the compliance. It should be clear from Fig. 10 that this most certainly is not a constant for collapsible tubes. The compliance attains a maximum at a value of transmural pressure slightly greater than that where the walls touch. This maximum is larger for tubes whose resting shape is more nearly circular. Since the compliance is always finite and positive, the area must be a monotonic function of the transmural pressure.

Thus, given a transmural pressure, there is only one area that the cross-section may have, and vice versa.

The behavior of the stress is an interesting topic. It was mentioned above that this in general is not constant. There are, in fact, situations where it will have a different sign at different points on the circumference. As an example, consider a shape such as is shown in Fig. 7 for $P = -4$. One quadrant of this is sketched in Fig. 13. If the equation for the stress, 10, is rewritten in cylindrical coordinates, it has the form:

$$\sigma = \frac{p}{h} r^2 \dot{\theta}. \tag{32}$$

In general, h and r^2 must be positive, and in the case being discussed, p is negative. Therefore the sign of σ_t will be opposite to that of $\dot{\theta}$ at all points. In Fig. 14, the area designated as a has $\dot{\theta}$ positive, so that the stress there is negative; i.e., the wall is under compression. In the area designated as b, just the opposite is true; θ decreases as the arc length increases, so that $\dot{\theta}$ is negative there. Thus, the stress in b is positive, and the wall is under tension. In c the angle θ is identically zero; so is $\dot{\theta}$, and hence the stress in this area must be identically zero.

The information presented in this paper provides a basis for analyzing the flow of fluid in collapsible tubes, and has direct application to venous hemodynamics. Knowing the behavior of the cross-sectional area as a function of the transmural pressure provides the basis for the design of a mathematical analogue for a short section of vein which takes into account the collapsibility of the tube, as well as the transmission-line effects. A calculation of the pressure-flow relationship in veins leading to such a mathematical analogue has been published by Kresch and Noordergraaf (1969). The collapse phenomenon of veins implies the presence of nonlinearities in the pressure vs. flow relationship so obtained which are of sufficiently large magnitude to preclude their being ignored. Thus, an electric analogue of a segment of vein, such as that proposed by Kresch and Noordergraaf (1969) which consists of nonlinear time-varying circuit elements, is both difficult to design and expensive to construct. Since a digital computer can handle a nonlinear problem as easily as a linear one, an analogue in the form of a computer program may be a good way to model several segments of a vein; however, an attempt to model the whole circulatory system on a digital computer may exceed the capabilities of modern-day computers because of the large number of variables in the system. It is possible that the use of hybrid techniques may prove to be a fruitful approach, in which the analogue computer can be used for the real-time calculations, and the digital computer can be used to perform the nonlinear calculations and control the parameters in the analogue computer. Whatever approach is taken, however, it is hoped that the information provided in this paper will be useful in modeling the venous system, and, ultimately, lead to a better understanding of the human circulatory system as a whole.

Dr. Noordergraaf, on leave from the University of Pennsylvania, is presently at the Department of Cardiology, Medical School of Rotterdam, Rotterdam, and the Laboratory for Applied Physics, Institute of Technology, Delft, The Netherlands.

This work was done at the University of Pennsylvania under U. S. Public Health Service grants HE 10,330 and 2 T01 GM-00606.
The Medical School Computer Facility of the University of Pennsylvania, which was used for some of the computations, is supported by National Institutes of Health grant FR 15.

Received for publication 5 May 1971 and in revised form 7 September 1971.

BIBLIOGRAPHY

ANLIKER, M., W. I. ASTLEFORD, and E. OGDEN. 1967. *Proc. Annu. Conf. Eng. Med. Biol.* **9:** 11.2.
ATTINGER, E. O. 1968. *In* Advances in Biomedical Engineering and Medical Physics. S. N. Levine, editor. Interscience Publishers, New York. **1.**
ATTINGER, E. O. 1969. *I.E.E.E. (Inst. Elec. Electron. Eng.) Trans. Bio-Med. Eng.* **BME16:** 253.
BRECHER, G. A. 1956. Venous Return. Grune & Stratton, Inc., New York.
BRECHER, G. A. 1969. *I.E.E.E. (Inst. Elec. Electron. Eng.) Trans. Bio-Med. Eng.* **BME16:**236.
CONRAD, W. A. 1969. *I.E.E.E. (Inst. Elec. Electron. Eng.) Trans. Bio-Med. Eng.* **BME16:**284.
COUCH, R. P. 1966. A model for the renal blood flow regulating mechanism. M.S. Thesis. Air Force Institute of Technology, Air University, Wright-Patterson Air Force Base, Ohio.
FRANKLIN, K. J. 1937. A Monograph on Veins. Charles C. Thomas, Publisher, Springfield, Ill.
HARVEY, W. 1628. *Exercitatio Anatomica de Motu Cordis et Sanguinis in Animalibus*, 1931. English translation by C. D. Leake. Charles C Thomas, Publisher, Springfield, Ill.
HOLT, J. P. 1969. *I.E.E.E. (Inst. Elec. Electron. Eng.) Trans. Bio-Med. Eng.* **BME16:**274.
KATZ, A. I., and Y. CHEN. 1970. *Proc. Annu. Conf. Eng. Med. Biol.* **12:** 12.
KRESCH, E. 1968. Design of a nonlinear electrical model for veins. Ph.D. Dissertation. University of Pennsylvania, Philadelphia.
KRESCH, E., and A. NOORDERGRAAF. 1969. *I.E.E.E. (Inst. Elec. Electron. Eng.) Trans. Bio-Med. Eng.* **BME16:**296.
MORENO, A. H., A. I. KATZ, L. D. GOLD, and R. V. REDDY. 1970. *Circ. Res.* **27:**1069.
REDDY, R. V., A. NOORDERGRAAF, and A. H. MORENO. 1970. *Proc. Annu. Conf. Eng. Med. Biol.* **12:**15.
WIGGERS, C. J. 1956. Foreword in Brecher, G. A. Venous Return. Grune & Stratton, Inc., New York.
WOOD, J. E. 1965. The Veins. Little, Brown and Company, Boston. 1st edition.